

# BRAIN TISSUE VOLUMES ESTIMATED FROM MAGNETIC RESONANCE SCANS IN PEDIATRIC HYDROCEPHALUS

Michael E. Brandt<sup>1</sup>, Jack M. Fletcher<sup>2</sup> and Larry A. Kramer<sup>3</sup>

<sup>1</sup>Center for Computational Biomedicine, University of Texas Health Science Center-SHIS, Houston, TX, USA

<sup>2</sup>Department of Developmental Pediatrics, University of Texas Medical School, Houston, TX, USA

<sup>3</sup>Department of Radiology, University of Texas Medical School, Houston, TX, USA

**Abstract**—Brain tissue volumetry from MRI scans was performed on a group of 28 children with shunted hydrocephalus (SH) and 14 neurologically-normal (NN) children. In the SH group increased cerebrospinal fluid (CSF) volumes were found in the posterior (postcallosal) and midline (pericallosal) regions in both hemispheres, but not anterior (precallosal) regions. There were corresponding reductions in both gray and white matter volumes in postcallosal and pericallosal regions. These results parallel animal studies showing that hydrocephalus is associated with loss of white matter and gray matter. The amount of loss is related to the degree of fine motor and memory deficits commonly observed in children with hydrocephalus.

**Keywords** – Hydrocephalus, MRI, brain tissue, volumetrics

## I. INTRODUCTION

Hydrocephalus in children is a dynamic brain disorder associated with increased volume of cerebrospinal fluid (CSF) due to obstruction of its flow. This leads to damage of various brain structures and is associated with a variety of neurobehavioral deficits. It can be caused by congenital malformations, hemorrhage, tumors, or infectious diseases. It can cause thinning of the cortical mantle and destruction of the corpus callosum (CC), the major connecting pathway between the two hemispheres of the brain. Myelinated brain structures are affected leading to loss of both major projection fibers and white matter in the occipital lobes. Hydrocephalus is also associated with a variety of neurobehavioral deficits, those in fine motor skills most pronounced. Studies of intellectual development typically show poorer nonverbal than verbal performance. Deficits in a variety of higher order cognitive skills involving memory, discourse production and comprehension, and attention are also apparent. Here, we performed brain MRI volumetry in children with shunted hydrocephalus (SH) and neurologically normal (NN) children (for review and details see [1]).

## II. METHODOLOGY

### A. Participants

Twenty-eight children with SH and 14 NN children were studied. The children with SH varied according to etiology, including 15 with spina bifida meningocele, 9 with aqueductal stenosis, and 4 premature birth with intraventricular hemorrhage. The two groups were comparable in age (SH group mean $\pm$ sd = 128 $\pm$ 31; NN = 139 $\pm$ 27 months), gender, ethnicity, and socioeconomic status ( $p < 0.05$ ). Diagnosis was based on the radiologist's review of

the MRI and medical records using standard clinical criteria. Children were excluded if they had another neurological disorder unrelated to shunting (including head injury and uncontrolled epilepsy), severe psychiatric disorder (autism, childhood psychosis), uncorrected sensory disorder, cerebral palsy, or IQ scores (verbal and performance) less than 70.

### B. MRI Acquisition

Whole brain MR scans were obtained using a GE Signa system (Milwaukee, WI) with a 1.5 Tesla superconducting magnet. A T2-weighted (T2W) coronal sequence (accentuating CSF) of contiguous 5 mm images, and a T1-weighted (T1W) coronal sequence (accentuating gray and white matter) of 5 mm contiguous images were obtained. CSF, gray and white matter volumes were computed from these two sequences.

### C. Scan Preprocessing

Analysis was performed on SGI and Sun workstations using software developed by us. Each sequence was intensity normalized and reformatted so that voxel dimensions were isotropic. The T1W and T2W scans for each subject were co-aligned by identifying up to five anatomic landmarks in each, including the anterior and posterior commissures, superior colliculi, and genu and splenium of the CC. In the SH group some of these landmarks were damaged/distorted so co-alignment was manually verified before proceeding. The two scan volumes were then centered within their own 256 cubic voxel bounding volume and convolved with a nonlinear anisotropic diffusion filter [2]. This filter sharpened areas of high intensity gradient (along structure borders) and smoothed regions of low-intensity gradient (inside tissue regions). From the T2W volume, another program was used to “extract” the cerebrum using both interactive intensity thresholding and manual delineation on a per slice basis. The region was then filled automatically to its borders, thereby defining an image mask. The hemispheres were separated by drawing a line along the interhemispheric fissure. Whole brain volume was then computed as the sum of the filled regions across the image slices. This masked volume thus identified the specific voxels to be included in the following segmentation analysis.

### D. Scan Segmentation and Derived Measures

We performed fuzzy cluster analysis to obtain whole and regional brain tissue volumes. Our procedure is based on the fuzzy c-means (FCM) algorithm [3] applied separately to

T1W and T2W volumes. The number of tissue groups (clusters) can be either exactly specified by the operator or estimated in the analysis procedure. We use the CSF volume computed from the T2W scan, and gray and white matter volumes from the T1W scan. Based on empirical experience gained over the years, we use randomized cluster initialization, we set the “fuzziness” parameter to an intermediate level ( $m = 3/2$ ), the number of clusters to 3 in the T2W scan (white, gray, CSF) and 5 in the T1W (white, CSF, and 3 gray matter subgroups). After a first pass clustering of each volume, we perform a validity-based cluster split-and-merge (VBSM) procedure on the solution [4]. The validity measure used is the ratio of cluster compactness (intracluster variance) to intercluster distance (mean distance between centroids). This ratio is minimized by splitting each cluster in turn and merging two others. Once the VBSM step is completed, the revised solution serves as an “optimized” cluster initialization to re-perform the FCM clustering. The validity of this last run may be better or worse than the initial FCM run. The better of the two is chosen as the accepted solution. This process can be repeated until stability is achieved, usually within a few runs. A solution volume is digitally constructed and can be compared onscreen alongside the preprocessed scan for final verification. The per subject solution provides both absolute and relative measures of CSF, white and (total) gray matter volumes within the cerebrum, each hemisphere, and pre-CC (frontal lobe), peri-CC (whole CC) and retro-CC (posterior to splenium) regions in each hemisphere [5].

### III. RESULTS

Fig. 1 is an example of the image analysis. We found the expected increased cerebrum volume in the SH group compared to NN's. After correcting for cerebrum size and age (by using relative tissue percentages) we found a statistically significant overall decrease (mean 2.4%) in both white and gray matter in the SH group, and increased percent of CSF (mean 4.6%). Means and standard deviations by region, tissue type and group are listed in Table I. MANOVA results showed that the SH group had 1) less CSF in both frontal (pre-CC) lobes, 2) no difference in pre-CC white or gray matter; 3) significantly less gray in the left peri-CC region (no difference in left peri-CC white); 4) significantly less white in right peri-CC (no difference in right peri-CC gray); 5) significantly greater peri-CC CSF; 6) significantly less gray AND white retro-CC; and 7) significantly increased CSF retro-CC.

### IV. DISCUSSION

Upon followup exploration of the SH group (by performing a group median split based on the ratio of pre-CC to retro-CC CSF %) it was determined that fine motor dexterity and memory performance are significantly poorer in the sub SH group with increased retro-CC CSF (and decreased white and

gray matter). This is just one example of the profound neurofunctional deficits associated with this disorder.

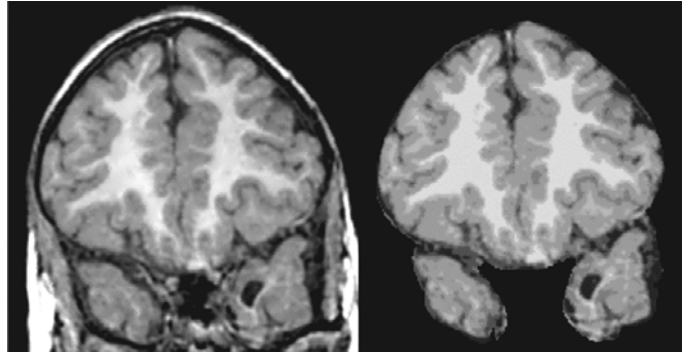


Fig. 1. Sample T1W coronal image from an SH child (left) showing the gray matter). This is just one example of the profound neurofunctional deficits associated with this disorder.

TABLE I. Regional brain tissue %'s by group; \* indicates  $p < 0.05$  or better significance based on multivariate analysis of variance (MANOVA).

Region, Tissue type		SH	NN
		mean $\pm$ sd (%)	mean $\pm$ sd (%)
<i>Left Pre-CC:</i>	Gray	67.7 $\pm$ 4.1	66.3 $\pm$ 2.2
	White	23.0 $\pm$ 4.6	22.5 $\pm$ 2.7
	CSF	*9.3 $\pm$ 3.2	11.2 $\pm$ 3.1
<i>Right Pre-CC:</i>	Gray	66.5 $\pm$ 3.9	64.9 $\pm$ 2.6
	White	25.2 $\pm$ 2.7	24.3 $\pm$ 2.7
	CSF	*8.4 $\pm$ 3.1	10.1 $\pm$ 2.7
<i>Left Peri-CC:</i>	Gray	*58.8 $\pm$ 5.3	62.3 $\pm$ 2.5
	White	26.5 $\pm$ 3.3	28.1 $\pm$ 2.4
	CSF	*14.7 $\pm$ 6.6	9.4 $\pm$ 1.3
<i>Right Peri-CC:</i>	Gray	59.6 $\pm$ 4.8	62.1 $\pm$ 2.8
	White	*26.8 $\pm$ 3.1	29.0 $\pm$ 2.8
	CSF	*13.6 $\pm$ 5.4	8.9 $\pm$ 1.1
<i>Left Retro-CC:</i>	Gray	*62.4 $\pm$ 5.7	65.2 $\pm$ 2.4
	White	*21.6 $\pm$ 3.4	25.5 $\pm$ 3.3
	CSF	*16.0 $\pm$ 7.0	9.3 $\pm$ 1.6
<i>Right Retro-CC:</i>	Gray	*64.3 $\pm$ 4.8	67.3 $\pm$ 2.0
	White	*19.6 $\pm$ 2.2	23.5 $\pm$ 3.0
	CSF	*16.1 $\pm$ 5.9	9.2 $\pm$ 2.2

### REFERENCES

- [1] J. Fletcher, T. Bohan, M. Brandt, L. Kramer, B. Brookshire, K. Thorstad, et al., “Morphometric evaluation of the hydrocephalic brain: Relationships with cognitive abilities,” *Child's Nerv. Sys.*, vol. 12, pp. 192-199, 1996.
- [2] G. Gerig, O. Kubler, R. Kikinis and F. Jolesz, “Nonlinear anisotropic diffusion filtering of MRI data,” *IEEE Trans. Med. Imag.*, vol. 11, pp. 221-232, 1992.
- [3] M. Brandt, T. Bohan, L. Kramer and J. Fletcher, “Estimation of CSF, white and gray matter volumes in hydrocephalic children using fuzzy clustering of MR images,” *Comp. Med. Imag. & Graph.*, vol. 18, pp. 25-34, 1994.
- [4] A. Bensaid, L. Hall, J. Bezdek, L. Clarke, M. Silbiger, J. Arrington, et al., “Validity guided (re)clustering with applications to image segmentation,” *IEEE Trans. Fuzz. Sys.*, vol. 4, pp. 112-123, 1996.
- [5] P. Filipek, “Structural variations in measures in the developmental disorders,” in *Developmental Neuroimaging*, R. Thatcher, G. Lyon, J. Rumsey, N. Krasnegor, Eds. San Diego: Academic Press, 1996, pp. 169-186.